PERGAMON

Mechanism and Machine Theory 35 (2000) 1689–1708

MECHANISM AND MACHINE THEORY

www.elsevier.com/locate/mechmt

Mathematical model and bearing contacts of the ZN-type worm gear set cut by oversize hob cutters

Hong-Sheng Fang [a,b], Chung-Biau Tsay [b,*]

[a] *MIRL, Industrial Technology Research Institute, Hsinchu, Taiwan, ROC*

[b] *Department of Mechanical Engineering, National Chiao Tung University, Hsinchu 30050, Taiwan, ROC*

Received 14 June 1999; accepted 31 March 2000

Abstract

The ZN-type oversize hob cutter for cutting of worm gears is investigated. The mathematical model of the ZN-type worm gear set is developed based on the cutting mechanism and hob cutter parameters. Influences of oversize hob cutter regrinding, worm-thread number and assembly errors on the bearing contacts and kinematical errors of the ZN-type worm gear set are investigated. A numerical example is given to demonstrate the bearing contacts and kinematical errors of the worm gear set.

1. Introduction

The worm gear set is composed of a worm and worm gear, and is one of the most important devices for transmitting torque between spatial crossed axes. Due to its high transmission ratio, low noise and compact structure, worm gear set is widely used in gear-reduction mechanisms. According to cutting methods and DIN standards, worm gear sets fall into one of four main types – ZA, ZN, ZE (or ZI) and ZK types. The worm-type hob cutter is one of the most popular cutting tools used in industry for worm gear manufacturing.

Characteristics and contact nature of the worm gear set have been investigated by many researchers. Their efforts improved the efficiency and working life time of worm gear sets. Wildhaber [1] was the first to use the surface curvatures to obtain an approximate tooth contact bearing diagram for worm gears cut by oversize hob cutters. Design criteria, classification and regrinding limitation of the oversize hob cutter were also investigated by Wildhaber [1]. Winter and Wilkesmann [5], Simon [11] and Bosch [8] proposed different methods of obtaining more

* Corresponding author. Tel.: +886-35-728-450; fax: +886-35-728-450.
E-mail address: cbtsay@cc.nctu.edu.tw (C.-B. Tsay).

0094-114X/00/$ - see front matter
PII: S0094-114X(00)00024-0

precise worm surfaces. Bär [4] investigated the basic geometry of worm surfaces, and also studied the grinding wheel surfaces and undercut problems. Pencil-type milling cutters and disk-type grinding wheels for producing worm surfaces were studied by Litvin [3]. Kin [9] investigated the limitation of worms to avoid undercutting, and also studied the envelope existence of contact lines. Colbourne [7] investigated undercutting, interference and non-conjugate contact of the ZK-type worm gear set. In his study, worm gear surfaces are obtained by considering the matting worm surface as a series of rack cutters in its axial section. Janninck [12] proposed a method for predicting the initial contact pattern and showed their results by applying a surface separation topological diagram over the entire worm gear surface. Colbourne [6] proposed a method for designing oversize hob cutters to cut worm gears. The contact surface separation topology concept was also adopted to show the results of his design. Litvin and Kin [2] also proposed a generalized tooth contact analysis (TCA) algorithm to determine the position of transfer points where an ideal contact line will turn into a real contact point. The influences of rotation axes misalignment and center-distance offset on the conjugate worm gear set were also investigated in their study. Kin [10] studied the surface deviations of the produced worm gear tooth surfaces due to cutting-edge deviations of hob cutters.

Theoretically, the ZN-type worm is cut by a straight-edged cutting blade, and the worm gear is produced by a worm-type hob cutter which is identical to the worm. The bearing contacts of the conjugate worm gear set are line contacts. However, oversize worm-type hob cutters are popularly used in industry for the worm gear manufacturing. The bearing contacts of the produced worm gear set are point contacts rather than line contacts. Due to the tooth surface elasticity under a load, the tooth surface of each contact gear will spread over an area, usually an elliptical area in the neighborhood of the contact points. The tooth surface bearing contacts are formed by a set of contact ellipses, moved over the tooth surfaces, in the process of gear meshing.

In this paper, the worm surface is cut with a straight-edged cutting blade on a lathe. The mathematical model of the ZN-type worm surface and the oversize hob cutter surface can be developed by considering the relationship of the cutting blade to the cutting mechanism. The ZN-type worm gear is produced by an oversize worm-type hob cutter. Therefore, the worm gear tooth equations can be obtained by simultaneously considering the locus equations of the oversize hob cutter together with the equation of meshing between the oversize hob cutter and the worm gear. The bearing contact and kinematical errors in the worm gear set are determined by applying the developed mathematical model of the worm gear set and TCA computer programs. Surface separation topology is also adopted to determine the shapes and locus of bearing contacts. Finally, a numerical example is given to demonstrate the determination of bearing contacts and kinematical errors in the ZN-type worm gear set. The influence of hob cutter regrinding, assembly errors and transmission ratio on the bearing contact and kinematical errors of the ZN-type worm gear set are also investigated in this paper. The proposed analysis procedures and the developed computer programs are most helpful in designing and analyzing worm gear sets, as well as in designing oversize hob cutters.

2. Mathematical model of the straight-edged cutting blade

The ZN-type worm is cut by a straight-edged cutting blade, and the cutting blade is placed on the groove normal section of the produced worm, as shown Fig. 1. Parameter β_1 is the lead angle

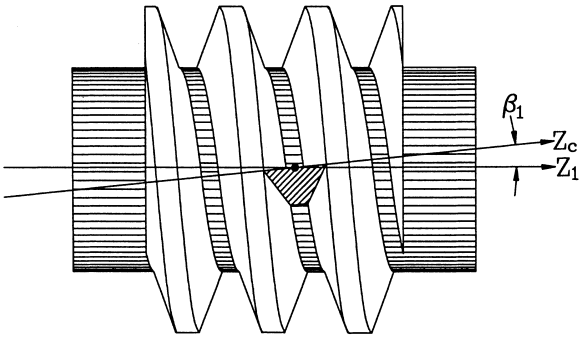

Fig. 1. Relationship between the cutting blade and worm.

of the worm. The surface equations of the straight-edged cutting blade, represented in the blade coordinate system $S_c(X_c, Y_c, Z_c)$, as shown in Fig. 2(b), can be expressed by:

$$\begin{aligned} x_c &= r_t + l_1 \cos\alpha_1, \\ y_c &= 0, \\ z_c &= \pm l_1 \sin\alpha_1, \end{aligned} \tag{1}$$

where l_1 is the surface parameter of the straight-edged cutting blade and $l_{min} \leqslant l_1 \leqslant l_{max}$. Design parameter α_1 is the half-apex blade angle formed by the straight-edged cutting blade and X_c-axis, as shown in Fig. 2(a) and (b). The plus sign of z_c expressed in Eq. (1) is associated with the right-hand cutter blade and the minus sign of z_c is associated with the left-hand cutter blade. The cutting blade width must equal the normal groove width of the produced worm, design parameter r_t can be obtained from Fig. 2(c) and (d), which can be represented as follows

$$r_t = \sqrt{r_1^2 - \frac{s_n^2}{4}\sin^2\beta_1} - \frac{s_n}{2\tan\alpha_1}, \tag{2}$$

where r_1 is the pitch radius and s_n the normal groove width of the produced worm.

3. Mathematical models of the ZN-type worm and oversize hob cutter

The ZN-type worm is cut by a straight-edged cutting blade placed on its groove normal plane. Therefore, the ZN-type worm surface is the locus of the cutting blade, and the worm surface geometry depends on the design parameters of the cutting blade and on machine-tool settings.

The ZN-type worm cutting mechanism can be simplified by considering the relative motion of a straight-edged cutting blade performing a screw motion along the worm rotation axis. As shown in Fig. 3, coordinate system $S_1(X_1, Y_1, Z_1)$ is associated with the worm surface, and coordinate system $S_f(X_f, Y_f, Z_f)$ is the reference coordinate system; Z_1-axis is the rotation axis of the worm.

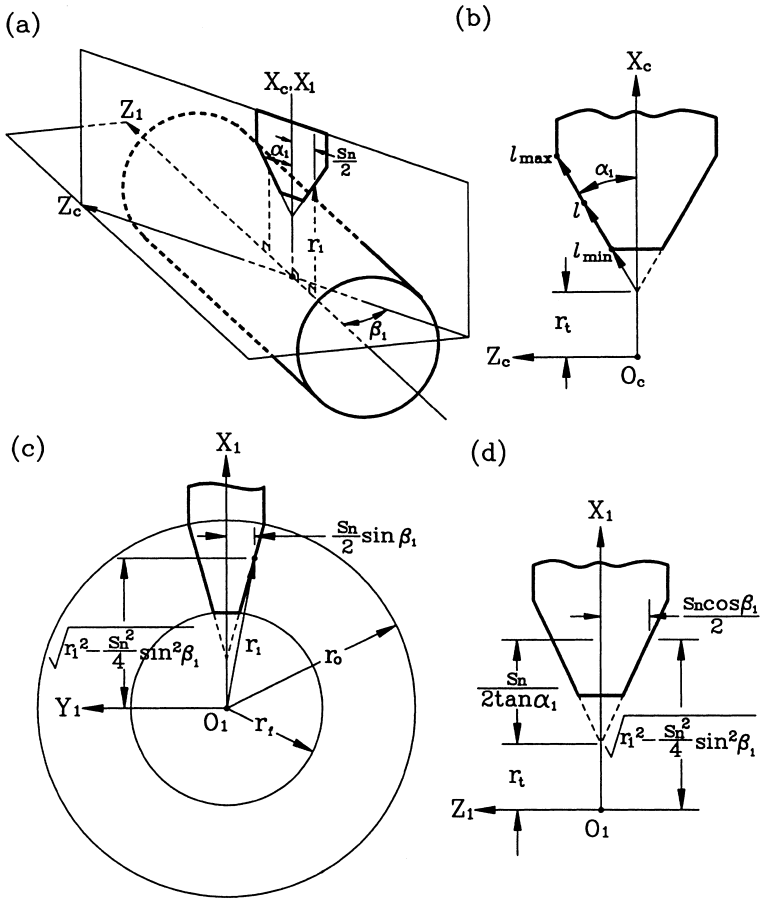

Fig. 2. Geometry of the straight-edged cutting blade.

The locus of the cutting blade can be represented in coordinate system S_1 by applying the following homogeneous coordinate transformation matrix equation

$$\begin{bmatrix} x_1 \\ y_1 \\ z_1 \\ 1 \end{bmatrix} = \begin{bmatrix} \sin\varphi_1 & \sin\varphi_1\cos\beta_1 & -\sin\varphi_1\sin\beta_1 & 0 \\ -\sin\varphi_1 & \cos\varphi_1\cos\beta_1 & \cos\varphi_1\sin\beta_1 & 0 \\ 0 & \sin\beta_1 & \cos\beta_1 & -P_1\varphi_1 \\ 0 & 0 & 0 & 1 \end{bmatrix} \begin{bmatrix} x_c \\ y_c \\ z_c \\ 1 \end{bmatrix}, \tag{3}$$

where parameter P_1 is the lead-per-radian revolution of the worm surface, and φ_1 the rotation angle of the worm in relative screw motion. Substituting Eq. (1) into Eq. (3), the ZN-type worm surface equation $\underset{\sim}{\boldsymbol{R}}_1$ can be obtained as follows:

$$\begin{aligned} x_1 &= A_1\cos\varphi_1 - B_1\sin\varphi_1, \\ y_1 &= -A_1\sin\varphi_1 - B_1\cos\varphi_1, \\ z_1 &= C_1 - P_1\varphi_1, \end{aligned} \tag{4}$$

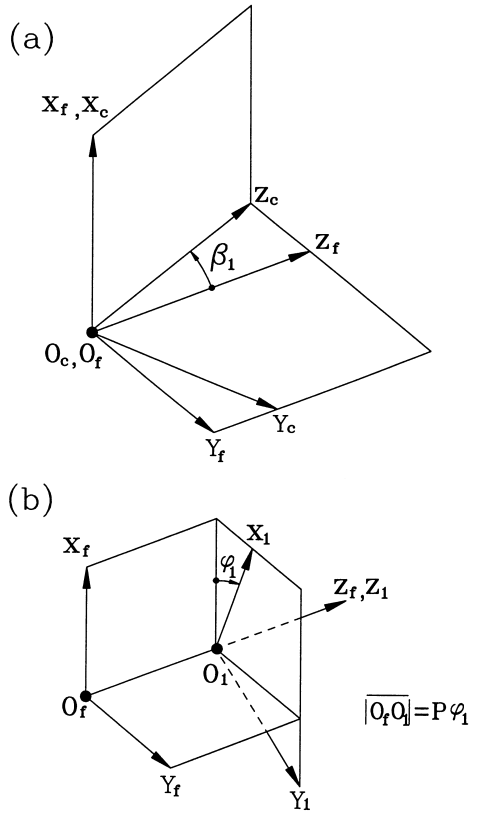

Fig. 3. Relationship between the worm and cutting blade coordinate systems.

where

$$A_1 = l_1 \cos\alpha_1 + r_{t1},$$
$$B_1 = \pm l_1 \sin\alpha_1 \sin\beta_1,$$
$$C_1 = \pm l_1 \sin\alpha_1 \cos\beta_1.$$

Because the worm surface must be limited between the outside radius r_o and root radius r_f of the worm, the upper and lower bounds of the design parameter l_1 can be determined by the following conditions:

$$x_1^2 + y_1^2 = r_o^2$$

i.e.

$$l_{\max} = \frac{\sqrt{(r_o^2 - r_t^2)\sin^2\alpha_1 \sin^2\beta_1 + r_o^2 \cos^2\alpha_1} - r_t \cos\alpha_1}{\sin^2\alpha_1 \sin^2\beta_1 + \cos^2\alpha_1}, \tag{5}$$

and

$$x_1^2 + y_1^2 = r_f^2$$

i.e.

$$l_{\min} = \frac{\sqrt{(r_f^2 - r_t^2)\sin^2\alpha_1 \sin^2\beta_1 + r_f^2 \cos^2\alpha_1} - r_t \cos\alpha_1}{\sin^2\alpha_1 \sin^2\beta_1 + \cos^2\alpha_1}. \tag{6}$$

The surface normal vector of the ZN-type worm thread surface can be obtained by applying the equation

$$\underset{\sim}{\boldsymbol{N}}_1 = \frac{\partial \underset{\sim}{\boldsymbol{R}}_1}{\partial l_1} \times \frac{\partial \underset{\sim}{\boldsymbol{R}}_1}{\partial \varphi_1}, \tag{7}$$

where

$$\frac{\partial \underset{\sim}{\boldsymbol{R}}_1}{\partial l_1} = \begin{bmatrix} \cos\alpha_1 \cos\varphi_1 \mp \sin\alpha_1 \sin\beta_1 \sin\varphi_1 \\ -\cos\alpha_1 \sin\varphi_1 \mp \sin\alpha_1 \sin\beta_1 \cos\varphi_1 \\ \pm \sin\alpha_1 \cos\beta_1 \end{bmatrix}$$

and

$$\frac{\partial \underset{\sim}{\boldsymbol{R}}_1}{\partial \varphi_1} = \begin{bmatrix} -(l_1 \cos\alpha_1 + r_t)\sin\varphi_1 \mp l_1 \sin\alpha_1 \sin\beta_1 \cos\varphi_1 \\ -(l_1 \cos\alpha_1 + r_t)\cos\varphi_1 \mp l_1 \sin\alpha_1 \sin\beta_1 \sin\varphi_1 \\ -P_1 \end{bmatrix}.$$

Substituting Eq. (4) into Eq. (7), the surface normal vector of the ZN-type worm thread, represented in coordinate system S_1, can be simplified as follows:

$$\begin{aligned} N_{x1} &= D_1 \sin\varphi_1 + E_1 \cos\varphi_1, \\ N_{y1} &= D_1 \cos\varphi_1 - E_1 \sin\varphi_1, \\ N_{z1} &= F_1, \end{aligned} \tag{8}$$

where

$$\begin{aligned} D_1 &= P_1 \cos\alpha_1 - l_1 \sin^2\alpha_1 \sin\beta_1 \cos\beta_1, \\ E_1 &= \pm(P_1 \sin\beta_1 + (l_1 \cos\alpha_1 + r_t)\cos\beta_1)\sin\alpha_1, \\ F_1 &= l_1(\sin^2\alpha_1 \cos^2\beta_1 - 1) - r_t \cos\alpha_1. \end{aligned}$$

The geometry of the ZN-type oversize hob cutter is actually a worm-type hob cutter, the surface and normal vector equations of the oversize hob cutter are the same as those of the ZN-type worm. Therefore, the surface and normal vector equations of the oversize hob cutter can be obtained by replacing the subscripts 1 with o in Eqs. (4) and (8).

4. Mathematical model of the worm gear surface

As mentioned therein before, in order to produce a point-contact worm gear set, the worm gear is usually cut by an oversize worm-type hob cutter. The mathematical model of the worm gear can be obtained by considering the locus of the oversize hob cutter together with the equation of meshing between the oversize hob cutter and worm gear. The cutting/meshing mechanism of a

worm gear set is shown in Fig. 4. The coordinate system, $S_1(X_1, Y_1, Z_1)$ is associated with the worm, $S_o(X_o, Y_o, Z_o)$ is associated with the oversize hob cutter and $S_2(X_2, Y_2, Z_2)$ is associated with the worm gear; and the fixed coordinate systems $S_w(X_w, Y_w, Z_w)$, $S_h(X_h, Y_h, Z_h)$ and $S_g(X_g, Y_g, Z_g)$ are

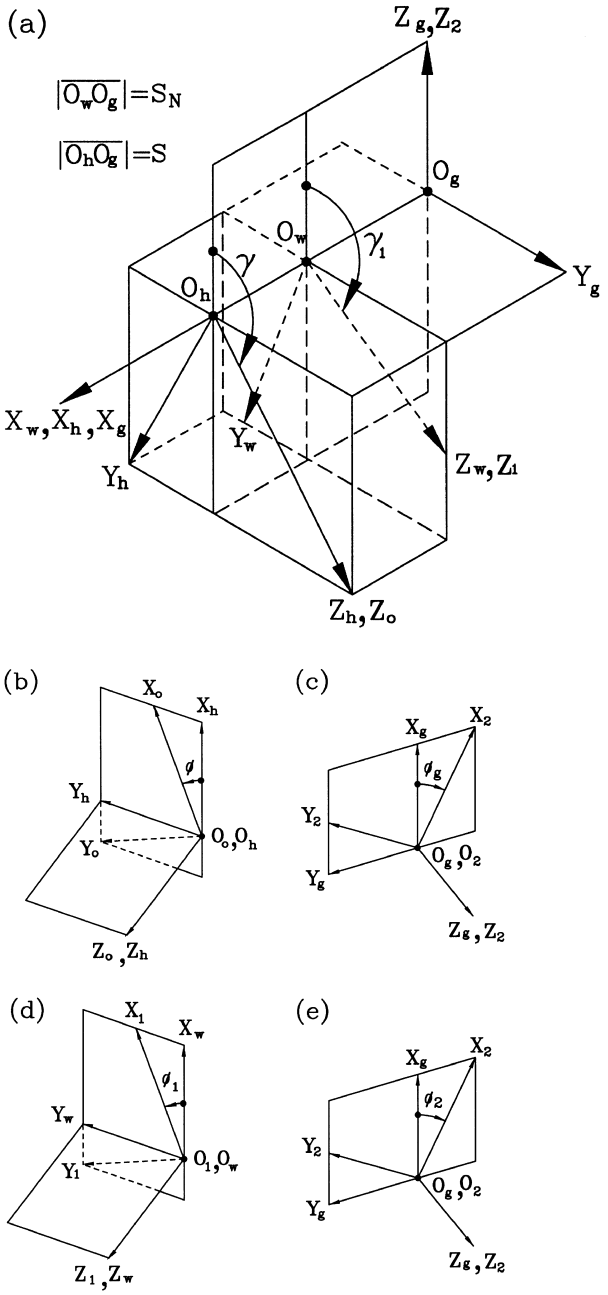

Fig. 4. Coordinate systems among the worm, worm gear and oversize hob cutter.

the reference coordinate systems for the worm, oversize hob cutter and worm gear, respectively. Axes Z_1, Z_o and Z_2 are the rotation axes of the worm, oversize hob cutter and worm gear, respectively. Parameters γ and γ_1, measured from Z_2-axis to Z_h-axis and Z_w-axis, are crossed setting-angles of the oversize hob cutter and worm, respectively. Parameters S and S_N are the shortest center-distances measured from the rotation axis of the worm gear to that of the oversize hob cutter and worm, respectively. The shortest center-distance can be expressed by equations:

$$S = r_o + r_2, \quad \text{and} \quad S_N = r_1 + r_2, \tag{9}$$

where r_o, r_1 and r_2 are the pitch radii of the oversize hob cutter, worm and worm gear, respectively. Rotation angles ϕ and ϕ_g, as shown in Fig. 4(b) and (c), are associated with the rotation angles of the oversize hob cutter and worm gear, respectively, during the cutting process. Rotation angles ϕ_1 and ϕ_2, shown in Fig. 4(d) and (e), are associated with the rotation angles of the worm and worm gear, respectively, during the meshing process. Since the oversize hob cutter and the produced worm gear remain in conjugation motion during the cutting process, rotation angles ϕ and ϕ_g can be related by the equation

$$\phi_g = \frac{N_h}{N_g}\phi, \tag{10}$$

where N_g and N_h are the tooth numbers of the worm gear and oversize hob cutter, respectively.

The locus of the oversize hob cutter represented in coordinate system S_2 can be obtained by applying the homogeneous coordinate transformation matrix equation

$$\underset{\sim}{\boldsymbol{R}}_2 = [M_{2o}]\underset{\sim}{\boldsymbol{R}}_o, \tag{11}$$

where $\underset{\sim}{\boldsymbol{R}}_2$ and $\underset{\sim}{\boldsymbol{R}}_o$ are the locus equations of the oversize hob cutters represented in coordinate systems $\underset{\sim}{S}_2$ and $\underset{\sim}{S}_o$, respectively. Actually, the geometry of the oversize hob cutter is a worm-type hob cutter, the surface equation can be obtained from Eq. (4) by replacing the subscripts 1 with o. Matrix $[M_{2o}]$ is the coordinate transformation matrix which transforms position vectors from coordinate system S_o to S_2, and is represented as follows

$$[M_{2o}] = \begin{bmatrix} a_{11} & a_{12} & \sin\phi_g \sin\gamma & -S\cos\phi_g \\ a_{21} & a_{22} & \cos\phi_g \sin\gamma & S\sin\phi_g \\ -\sin\phi\sin\gamma & -\cos\phi\sin\gamma & \cos\gamma & 0 \\ 0 & 0 & 0 & 1 \end{bmatrix}, \tag{12}$$

where

$$\begin{aligned} a_{11} &= \sin\phi\sin\phi_g\cos\gamma + \cos\phi\cos\phi_g, \\ a_{12} &= \cos\phi\sin\phi_g\cos\gamma - \sin\phi\cos\phi_g, \\ a_{21} &= \sin\phi\cos\phi_g\cos\gamma - \cos\phi\sin\phi_g, \\ a_{22} &= \cos\phi\cos\phi_g\cos\gamma + \sin\phi\sin\phi_g. \end{aligned}$$

Parameter γ represents the setting angle of the oversize hob cutter. Substituting Eqs. (4) and (12) into Eq. (11), the locus of the oversize hob cutter, represented in worm gear coordinate system S_2, is obtained as follows

$$
\begin{aligned}
x_2 &= [(A_o \sin(\phi - \varphi_o) - B_o \cos(\phi - \varphi_o)) \cos\gamma + (C_o - P_o\varphi_o) \sin\gamma] \sin\phi_g \\
&\quad + (A_o \cos(\phi - \varphi_o) + B_o \sin(\phi - \varphi_o) - S) \cos\phi_g, \\
y_2 &= [(A_o \sin(\phi - \varphi_o) - B_o \cos(\phi - \varphi_o)) \cos\gamma + (C_o - P_o\varphi_o) \sin\gamma] \cos\phi_g \\
&\quad - (A_o \cos(\phi - \varphi_o) + B_o \sin(\phi - \varphi_o)) - S) \sin\phi_g, \\
z_2 &= (C_o - P_o\varphi_o) \cos\gamma - (A_o \sin(\phi - \varphi_o) - B_o \cos(\phi - \varphi_o)) \sin\gamma,
\end{aligned} \tag{13}
$$

where parameters A_o, B_o and C_o are defined similar to those represented in Eq. (4) by changing the subscripts 1 with o. The surface normal vector of the worm gear, represented in coordinate system S_2, can be obtained by applying the vector transformation matrix equation

$$
\underset{\sim}{N}_2 = [L_{2o}]\underset{\sim}{N}_o, \tag{14}
$$

where $\underset{\sim}{N}_2$ and $\underset{\sim}{N}_o$ are surface normal vectors of the worm gear and oversize hob cutter, represented in coordinate systems S_2 and S_o , respectively. Normal vector $\underset{\sim}{N}_o$ can be obtained from Eq. (8) by replacing the subscripts 1 with o. Matrix $[L_{2o}]$ is the surface normal vector transformation matrix, transforming from coordinate system S_o to S_2, and it can be obtained by deleting the last column and last row of matrix $[M_{2o}]$ represented in Eq. (12). Therefore, the surface normal vector of the produced worm gear surface is expressed by:

$$
\begin{aligned}
N_{x2} &= [(D_o \cos(\phi - \varphi_o) + E_o \sin(\phi - \varphi_o)) \cos\gamma + n_z \sin\gamma] \sin\phi_g \\
&\quad - (D_o \sin(\phi - \varphi_o) - E_o \cos(\phi - \varphi_o)) \cos\phi_g, \\
N_{y2} &= [(D_o \cos(\phi - \varphi_o) + E_o \sin(\phi - \varphi_o)) \cos\gamma + n_z \sin\gamma] \cos\phi_g \\
&\quad + (D_o \sin(\phi - \varphi_o) - E_o \cos(\phi - \varphi_o)) \sin\phi_g, \\
N_{z2} &= n_z \cos\gamma - (D_o \cos(\phi - \varphi_o) + E_o \sin(\phi - \varphi_o)) \sin\gamma.
\end{aligned} \tag{15}
$$

Parameters D_o and E_o are defined similar to those represented in Eq. (8) by changing the subscripts 1 with o. During the cutting process, the oversize hob-cutter and worm gear surfaces remain conjugate motion and are in line contact at every moment. For the conjugate action, the hob cutter and produced worm gear surfaces are in continuous tangency during the cutting process. Therefore, the relative velocity between these two surfaces must lay on the common tangent plane. Hence, the following equation should be observed

$$
\underset{\sim}{N}_o \cdot \underset{\sim}{V}^{12}_o = 0, \tag{16}
$$

where $\underset{\sim}{N}_o$ is the surface common normal vector of matting surfaces and $\underset{\sim}{V}^{12}_o$ is the relative velocity of matting surfaces, represented in coordinate system S_o. Eq. (16) is known in the theory of gearing as the equation of meshing. The relative velocity between the hob cutter and worm gear surfaces, represented in coordinate system S_o, can be obtained by applying the equation

$$
\underset{\sim}{V}^{12}_o = (\underset{\sim}{\omega}_h - \underset{\sim}{\omega}_g) \times \underset{\sim}{R}_o + \underset{\sim}{\omega}_h \times \underset{\sim}{\mathbf{R}}, \tag{17}
$$

where $\underset{\sim}{R}_o$ is the position vector of any common contact point, represented in coordinate system S_o, as expressed in Eq. (4) by changing the subscripts 1 with o. ω_h and ω_g are the angular velocities of the hob cutter and worm gear, respectively. Position vector $\underset{\sim}{R}$ is measured from the origin of the

hob cutter coordinate system to any point on the rotation axis of the worm gear, represented in coordinate system S_o. Substituting Eqs. (4), (8), and (17) into Eq. (16), the equation of meshing of the oversize hob cutter and worm gear can be obtained as follows:

$$\begin{aligned}&\{E_oS\cos\gamma-[D_o(C_o-P_o\varphi_o)+B_oF_o]\sin\gamma\}m_{gh}\sin(\phi-\varphi_o)\\&\quad+\{D_oS\cos\gamma+[E_o(C_o-P_o\varphi_o)+A_oF_o]\sin\gamma\}m_{gh}\cos(\phi-\varphi_o)\\&\quad+(A_oD_o+B_oE_o)(1-m_{gh}\cos\gamma)+F_om_{gh}S\sin\gamma=0,\end{aligned}\tag{18}$$

where symbol m_{gh} is the rotation ratio of the worm gear and oversize hob cutter, and it can be expressed as follows

$$m_{gh}=\left|\frac{\omega_g}{\omega_h}\right|=\left|\frac{\phi_g}{\phi}\right|=\frac{N_h}{N_g}.\tag{19}$$

Since the equations of the ZN-type oversize hob cutter surface are obtained by the locus method, the equation of meshing between the hob cutter and the produced worm gear can always be derived in a close-form equation. Substituting the definitions of A_o, B_o, C_o, D_o, E_o and F_o represented in Eqs. (4) and (8) into Eq. (18), the closed-form equation of meshing between the oversize hob cutter and the worm gear can be expressed as follows:

$$l_o=\frac{1}{2\cdot a}\left(-b+\sqrt{b^2-4\cdot a\cdot c}\right),\tag{20}$$

where

$$\begin{aligned}a&=a_1\sin(\phi-\varphi_o)+a_2\cos(\phi-\varphi_o),\\b&=(b_1\varphi_o+b_2)\sin(\phi-\varphi_o)+(b_3\varphi_o+b_4)\cos(\phi-\varphi_o)+b_5,\\c&=(c_1\varphi_o+c_2)\sin(\phi-\varphi_o)+(c_3\varphi_o+c_4)\cos(\phi-\varphi_o)+c_5,\\a_1&=\pm m_{gh}\sin\alpha_o\sin\beta_o\sin\gamma,\\a_2&=m_{gh}\cos\alpha_o\sin\gamma,\\b_1&=-m_{gh}P_o\sin^2\alpha_o\sin\beta_o\cos\beta_o\sin\gamma,\\b_2&=\pm m_{gh}[(r_t\sin\beta_o-P_o\cos\beta_o)\sin\gamma+S\cos\gamma\cos\beta_o]\sin\alpha_o\cos\alpha_o,\\b_3&=\mp m_{gh}P_o\sin\alpha_o\cos\alpha_o\cos\beta_o\cos\gamma,\\b_4&=m_{gh}\left[(P_o\sin\gamma-S\cos\gamma)\sin^2\alpha_o\sin\beta_o\cos\beta_o+\left(1+\cos^2\alpha_o\right)r_t\sin\gamma\right],\\b_5&=\left(\sin^2\beta_o+\cos^2\alpha_o\cos^2\beta_o\right)\left(1-m_{gh}\cos\gamma\right)P_o+\left(\sin^2\alpha_o\cos^2\beta_o-1\right)m_{gh}S\sin\gamma,\\c_1&=m_{gh}P_o^2\cos\alpha_o\sin\gamma,\\c_2&=\pm(r_t\cos\beta_o-P_o\sin\beta_o)m_{gh}S\sin\alpha_o\cos\gamma,\\c_3&=\pm(r_t\cos\beta_o+P_o\sin\beta_o)m_{gh}P_o\sin\alpha_o\sin\gamma,\\c_4&=\pm\left(P_oS\cos\gamma+r_t^2\sin\gamma\right)m_{gh}\cos\alpha_o,\\c_5&=\pm\left[P_o\left(1-m_{gh}\cos\gamma\right)-Sm_{gh}\sin\gamma\right]r_t\cos\alpha_o.\end{aligned}$$

Therefore, the mathematical model of the worm gear surface cut with an oversize hob cutter can be obtained by considering Eqs. (13) and (20) simultaneously.

5. TCA of worm gear sets

TCA of the worm and worm gear can be simulated by considering the meshing mechanism of worm gear sets as shown in Fig. 4. If the worm rotates about its rotation axis through an angle ϕ_1, the worm gear will rotate about its rotation axis through an angle ϕ_2. Parameter S_N is the shortest distance between the worm axis Z_1 and worm gear axis Z_2, and γ_1 is the crossed setting-angle of these two axes.

To perform TCA on the worm gear set, position vectors and normal vectors of the matting worm and worm gear surfaces must be expressed in the same reference coordinate system, say coordinate system $S_w(X_w, Y_w, Z_w)$, as shown in Fig. 4(a). According to Fig. 4 and the coordinate transformation method, the position vector and normal vector of the worm surface, represented in coordinate system S_w, can be obtained as follows:

$$\begin{aligned} x_w^1 &= A_1 \cos(\phi_1 - \varphi_1) + B_1 \sin(\phi_1 - \varphi_1), \\ y_w^1 &= A_1 \sin(\phi_1 - \varphi_1) - B_1 \cos(\phi_1 - \varphi_1), \\ z_w^1 &= C_1 - P_1 \varphi_1, \end{aligned} \tag{21}$$

$$\begin{aligned} N_{yw}^1 &= E_1 \cos(\phi_1 - \varphi_1) - D_1 \sin(\phi_1 - \varphi_1), \\ N_{yw}^1 &= D_1 \cos(\phi_1 - \varphi_1) + E_1 \sin(\phi_1 - \varphi_1), \\ N_{zw}^1 &= N_{z1}. \end{aligned} \tag{22}$$

Similarly, the position vector and normal vector of the worm gear surface, represented in coordinate system S_w, are obtained as follows:

$$\begin{aligned} x_w^2 &= x_2 \cos\phi_2 - y_2 \sin\phi_2 + S_N, \\ y_w^2 &= (x_2 \sin\phi_2 + y_2 \cos\phi_2)\cos\gamma_1 - z_2 \sin\gamma_1, \\ z_w^2 &= (x_2 \sin\phi_2 + y_2 \cos\phi_2)\sin\gamma_1 + z_2 \cos\gamma_1, \end{aligned} \tag{23}$$

$$\begin{aligned} N_{xw}^2 &= N_{x2} \cos\phi_2 - N_{y2} \sin\phi_2, \\ N_{yw}^2 &= \left(N_{x2} \sin\phi_2 + N_{y2} \cos\phi_2\right)\cos\gamma_1 - N_{z2} \sin\gamma_1, \\ N_{zw}^2 &= \left(N_{x2} \sin\phi_2 + N_{y2} \cos\phi_2\right)\sin\gamma_1 + N_{z2} \cos\gamma_1. \end{aligned} \tag{24}$$

In the meshing process, worm and worm gear surfaces are in continuous tangency at every contact point. Therefore, the following meshing criteria must be observed at every contact point: (1) position vectors of the worm surface $\underset{\sim}{\mathbf{R}}_w^1$ and worm gear surface $\underset{\sim}{\mathbf{R}}_w^2$ are equal at every contact point; (2) the normal vector of the worm surface $\underset{\sim}{\boldsymbol{N}}_w^1$ must be parallel to the normal vector of the

worm gear surface $\underset{\sim}{N}^2_{\mathrm{w}}$. Based on Eqs. (21)–(24) and the above mentioned meshing criteria, a system of five independent equations can be obtained:

$$A_1 \cos(\phi_1 - \varphi_1) + B_1 \sin(\phi - \varphi_1) - x_2 \cos\phi_2 + y_2 \sin\phi_2 - S_N = 0, \tag{25}$$

$$A_1 \sin(\phi_1 - \varphi_1) - B_1 \cos(\phi_1 - \varphi_1) - (x_2 \sin\phi_2 + y_2 \cos\phi_2)\cos\gamma_1 + z_2 \sin\gamma_1 = 0, \tag{26}$$

$$C_1 - P_1\varphi_1 - (x_2 \sin\phi_2 + y_2 \cos\phi_2)\sin\gamma_1 - z_2 \cos\gamma_1 = 0, \tag{27}$$

$$N^1_{y\mathrm{w}} N^2_{z\mathrm{w}} - N^1_{z\mathrm{w}} N^2_{y\mathrm{w}} = 0 \tag{28}$$

$$N^1_{x\mathrm{w}} N^2_{z\mathrm{w}} - N^1_{z\mathrm{w}} N^2_{x\mathrm{w}} = 0. \tag{29}$$

The system equations above contain six unknowns $l_1, \varphi_1, \varphi_{\mathrm{o}}, \phi_1, \phi_2$ and ϕ. We may consider the worm rotation angle ϕ_1 as an input, and the other five unknowns can thus be determined. By solving the system equations (25)–(29) and the equation of meshing (20) simultaneously, the coordinates of every instantaneous contact point can be determined. The kinematic errors of the worm gear $\Delta\phi_2$ are defined and calculated by the following equation

$$\Delta\phi_2 = (\phi_2 - \phi_{20}) - \frac{N_1}{N_2}(\phi_1 - \phi_{10}), \tag{30}$$

where ϕ_{10} and ϕ_{20} are the rotation angles of the worm and worm gear, respectively, at some reference contact points. N_1 and N_2 are the teeth number of worm and worm gear, respectively.

6. Surface separation topology

In the matting process, worm and worm gear surfaces are tangent to each other at every instantaneous contact points. Therefore, a common tangent plane to the matting surfaces can be found at any contact point. In order to measure the separation value between two surfaces, surface coordinates of the worm and worm gear must be transformed to the common tangent plane, and the separation value of two matting surfaces can be measured along the normal direction of the tangent plane. Based on the prescribed separation value, the contour of contact ellipses can be obtained by applying a contouring algorithm.

7. Numerical example

A worm gear set with a transmission ratio of 1:33 was chosen for the demonstrative example. Some major design parameters of the worm gear set are given as follows: (1) Tooth number of the worm and oversize hob cutter $N_1 = 1$ tooth; (2) Module of the worm and oversize hob cutter $m = 8.5$ mm/tooth; (3) Crossed setting-angle of the worm $\gamma_1 = 90°$; (4) Pitch diameter of the worm $d_1 = 79.5$ mm; (5) Half-apex blade angle of the straight-edged cutting blade is $\alpha = 20°$; (6) Pitch diameter of the oversize hob cutter $d_1 = 85.00$ mm. The oversize hob cutter is based on the concept that the tooth widths of the worm and hob cutter are equal in their normal sections on the pitch cylinder. In order to satisfy this criterion, the setting angle γ of the oversize hob cutter in

the cutting process must be set smaller than that of the worm in the meshing process (i.e., angle γ_1), as shown in Fig. 4(a), and it can be expressed by:

$$\gamma = \gamma_1 - \beta_1 + \beta_o = 89°35'59'', \tag{31}$$

where β_1 and β_o are the lead angles of the worm and oversize hob cutter, respectively. According to the developed mathematical model of the worm gear set, a three-dimensional computer graphic of the ZN-type worm gear set is shown in Fig. 5. Based on the developed mathematical model of the worm gear set, the contact surface topology method and TCA computer simulation programs, the bearing contact of worm gear sets can be obtained. Fig. 6(a)–(c) show the bearing contacts on the worm gear surfaces when pitch diameters of the oversize hob cutter are 85.00 mm (6.92% oversize), 80.00 mm (0.63% oversize) and 79.50 mm (without oversize), respectively. It is worth of mentioning that line contact is occurred when the pitch diameter of hob cutters is reground to 79.50 mm, which is equal to the pitch diameter of the worm. In this case, the worm gear set becomes a conjugate kinematic pair rather than a pseudo-conjugate gear pair, and the kinematical error is zero. In this example, the separation value of the bearing contours is chosen as 0.00635 mm which is the size of coating particles used in the rolling-test experiments. Fig. 7 shows kinematical errors of the worm gear set, with pitch diameters of oversize hob cutter 85.00 and 80.00 mm, are 2.76 and 0.27 arc-s, respectively. The influences of assembly errors on the ZN-type worm gear set are investigated when the worm gear is cut by an oversize hob cutter with pitch diameter of 85.00 mm and pitch diameter of the matting worm is 79.50 mm. Fig. 8(a) and (b) show the bearing contacts of the worm gear set with 0.42 mm (0.233% center-distance) and -0.42 mm (-0.233% center-distance) center-distance offsets, respectively. The kinematical errors of 0.233% and -0.233% center-distance offsets are 2.95 and 2.50 arc-s, respectively, as shown in Fig. 9. Fig. 10(a) and (b) show the bearing contacts of the worm gear set with axes misalignments of 0.25° and -0.49°, respectively. Fig. 11 shows the

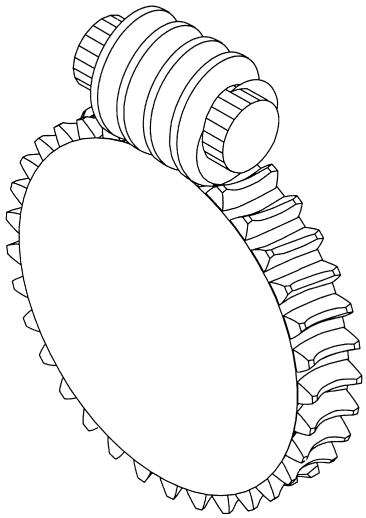

Fig. 5. Three-dimensional computer graphic of the ZN-type worm gear set.

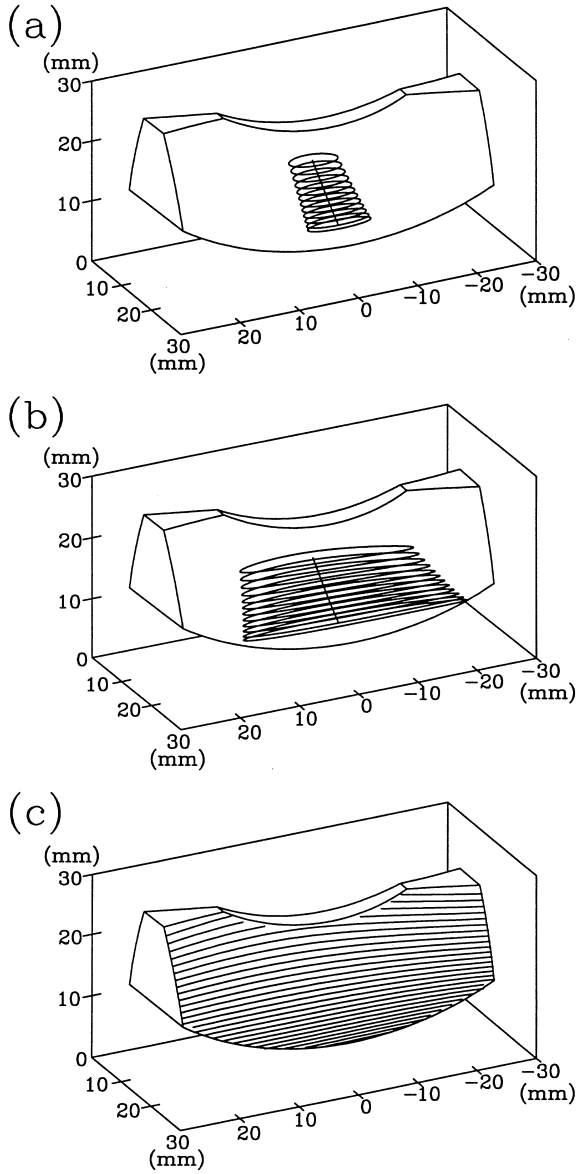

Fig. 6. Bearing contacts and contact paths of the ZN-type worm gear set under different oversize hob cutter pitch diameters.

kinematical errors are 2.91 and 2.97 arc-s for the worm gear set with axes misalignments of 0.25° and −0.49°, respectively. Finally, the bearing contact and kinematical errors of the worm gear set due to the worm-thread number are shown in Figs. 12 and 13. Fig. 12(a) shows the bearing contacts of two threads worm (rotation ratio 2/33) while Fig. 12(b) shows the three threads worm (rotation ratio 3/33).

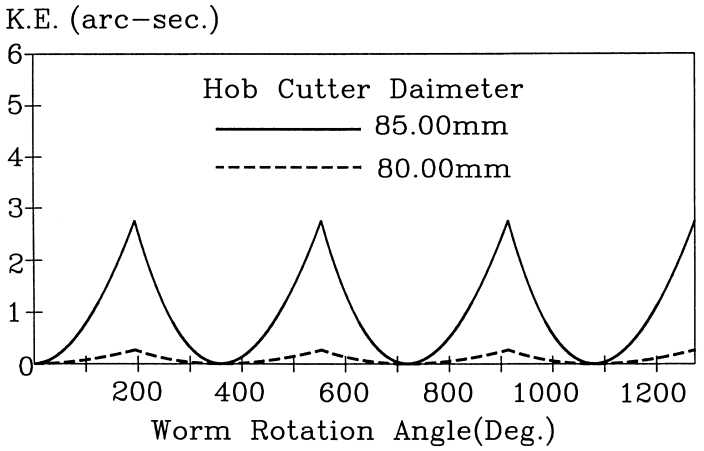

Fig. 7. Kinematical errors of the ZN-type worm gear set under different oversize hob cutter pitch diameters.

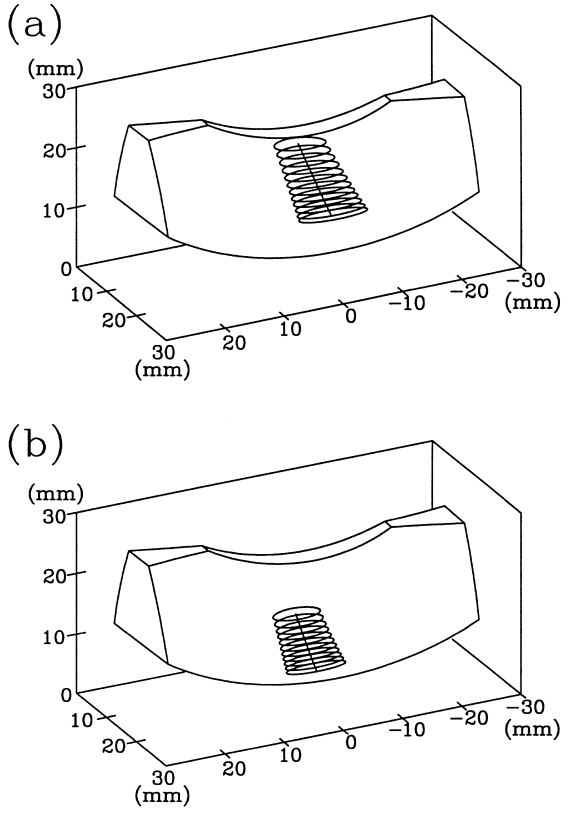

Fig. 8. Bearing contacts and contact paths of the ZN-type worm gear set under different center-distance offset assemblies.

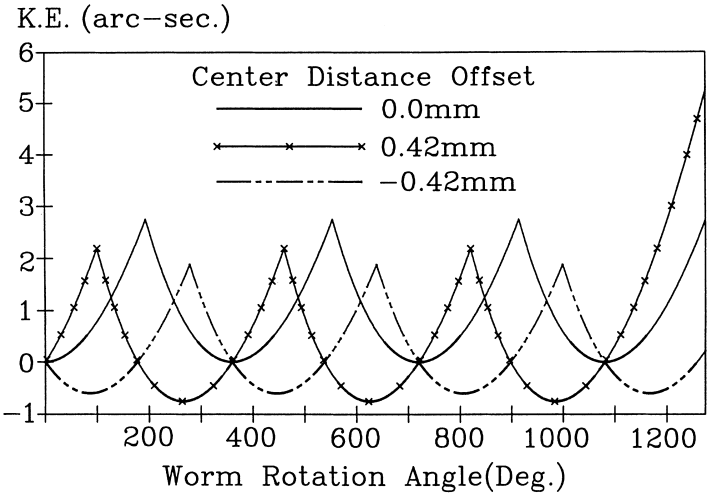

Fig. 9. Kinematical errors of the ZN-type worm gear set under different center-distance offset assemblies.

8. Discussion

When the oversize hob cutter is reground to a smaller pitch diameter, the contact ellipse of the produced worm gear set will be spread over a longer contact shape, as shown in Fig. 6. This phenomenon complies with the fact that line contact will occur and kinematical error is zero for the conjugate matting worm gear pair when the pitch diameter of the oversize hob cutter is decreased to equal to that of the worm. As shown in Fig. 7, the level of kinematical errors of the produced worm gear set will be lower if a small pitch diameter of oversize of hob cutter is used to cut the worm gear. As demonstrated in Fig. 6(a), if the pitch diameter of oversize hob cutter is larger than 85.00 mm, the area of bearing contacts will be too small to carry a heavy load. Meanwhile, if the pitch diameter of oversize hob cutter is smaller than 80.00 mm, edge contact will be occur, and edge failure may happen. For these reasons, the working life of the hob cutter can be ranged oversize from 6.92% to 0.63% pitch diameter.

If the worm gear set has 0.233% center-distance offset, bearing contacts will be located near the upper worm gear surface. On the contrary, if the worm gear set has −0.233% center-distance offset, bearing contacts will be located near the bottom worm gear surface, as shown Fig. 8. In order to avoid the edge contact on worm gear surface, an admissible assembly center-distance offset can be limited in the range of 0.233% and −0.233% center-distance variation. If the worm gear set has 0.25° rotation axes misalignment, bearing contacts will be located near the right side of worm gear surface and spread over a longer contact area. If the worm gear set has −0.49° rotation axes misalignment, bearing contacts will be located near the left side of worm gear surface, as shown in Fig. 10, and this is the critical case to avoid jumping in its motion curve. To avoid the edge contact and impact contact on worm gear surface, an admissible assembly axes misalignment can be limited between the range of 0.25° and −0.49°.

Comparing Fig. 6(a) with Fig. 12, the contact path will become more spiral while the worm-thread number is increased form one to three threads. As shown in Fig. 13, kinematical errors of

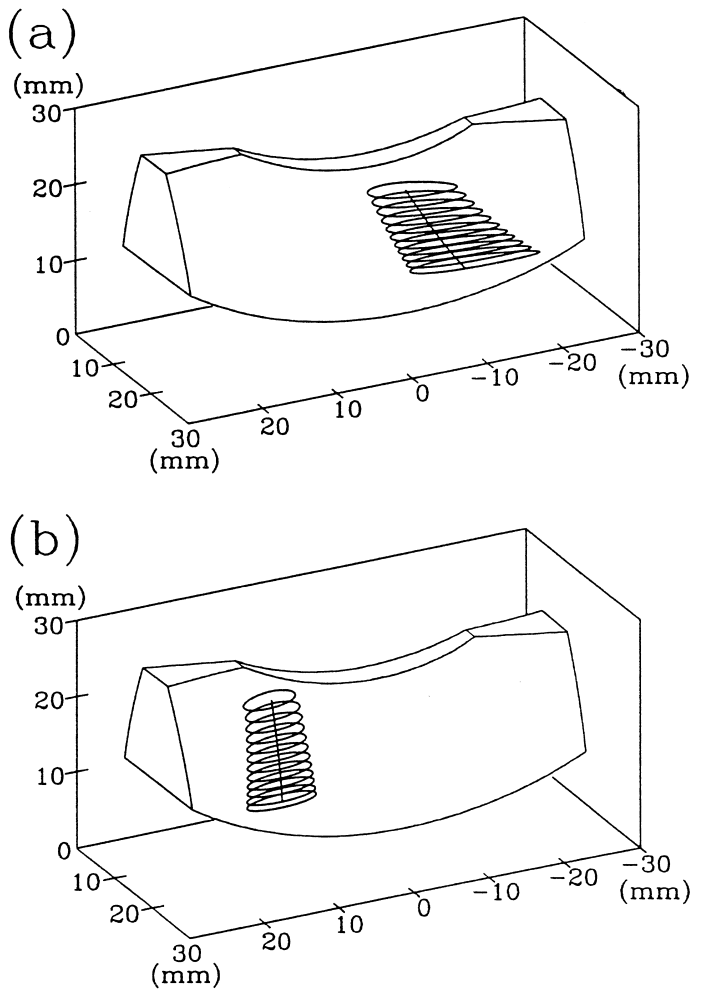

Fig. 10. Bearing contacts and contact paths of the ZN-type worm gear set under different axes misalignments.

worm gear set with two and three threads worm are 10.76 and 23.56 arc-s, respectively. In practice, these kinematical errors are too large to be accepted.

9. Conclusion

Based on the developed mathematical model, the tooth surfaces of the ZN-type worm and worm gear have been obtained. By applying the TCA technique, the bearing contact and kinematical errors due to the regrinding of oversize hob cutter have been investigated. The profile and dimension of contact ellipses are very important to the stress and lubrication analyses of the worm gear set, and also helpful to the estimation of working life of the oversize hob cutter. The influence and limitation of assembly errors can also be obtained by the TCA computer simulation. Since the

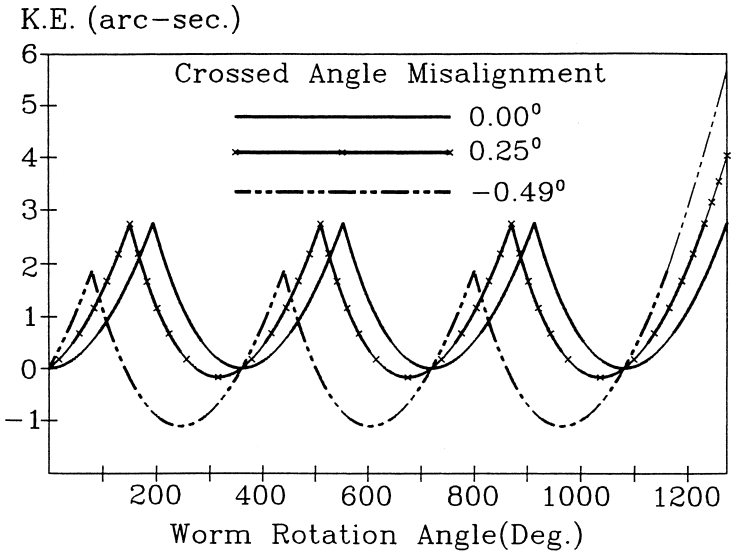

Fig. 11. Kinematical errors of the ZN-type worm gear set under different axes misalignments.

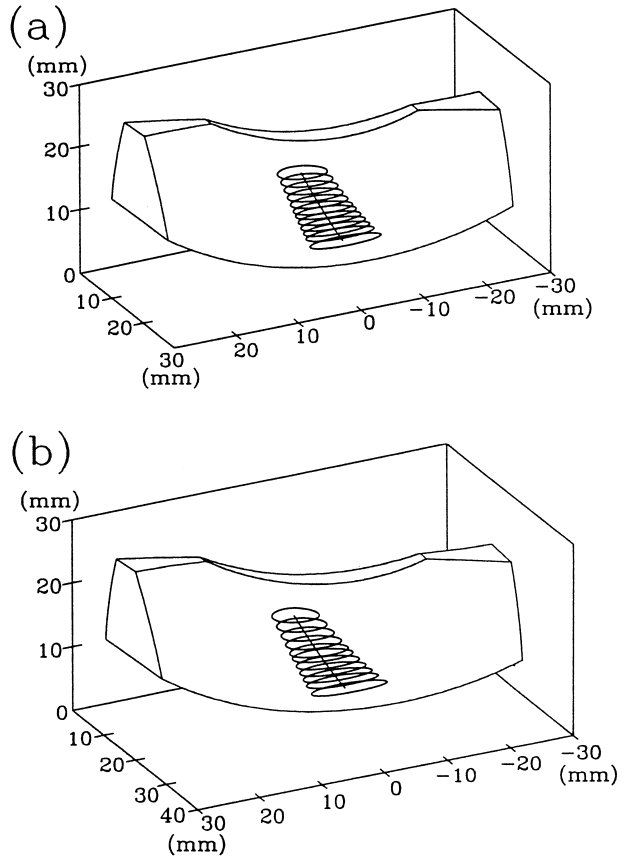

Fig. 12. Bearing contacts and contact paths of the ZN-type worm gear set under different worm-thread number.

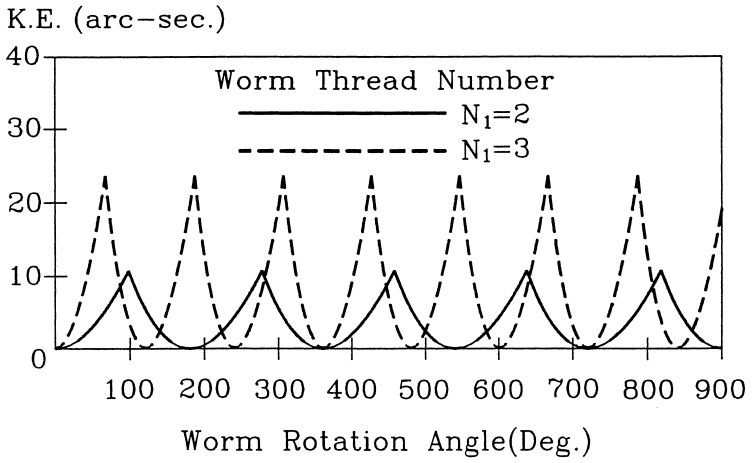

Fig. 13. Kinematical errors of the ZN-type worm gear set under different worm-thread number.

proposed worm and worm gear surfaces are not conjugate surfaces, kinematical errors in the worm gear set exist even under ideal assembly conditions. But the kinematical errors in the worm gear set describe a parabolic curve, this means no jump contact in the meshing cycle. Finally, the influence of contact ratio on bearing contacts and kinematical errors have also been investigated in this paper.

Acknowledgements

The authors are grateful to the National Science Council of the ROC for their grant. Part of this work was performed under the contract No. NSC-84-2212-E009-016.

References

[1] E. Wildhaber, A New Look at Wormgear Hobbing, American Gear Manufactures Association Conference, Virginia, 1954.
[2] F.L. Litvin, V. Kin, ASME J. Mech. Design 114 (1992) 313.
[3] F.L. Litvin, Gear Geometry and Applied Theory, Prentice-Hall, Englewood Cliffs, NJ, 1994, p. 642.
[4] G. Bär, Computers and Graphics 14 (1990) 405.
[5] H. Winter, H. Wilkesmann, J. Mech. Design 103 (1981) 73.
[6] J.R. Colbourne, The Use of Oversize Hobs to Cut Worm Gears, American Gear Manufactures Association Conference, Virginia, 1989.
[7] J.R. Colbourne, Undercutting in Worm and Worm-gears, American Gear Manufactures Association Conference, Virginia, 1993.
[8] M. Bosch, Economical Production of High Precision Gear Worms and Other Thread Shaped Profiles by Means of CNC-Controlled Worm and Thread Grinding Machines, Klingelnberg Publication, Germany, 1988, p. 3.
[9] V. Kin, Gear Technology 7 (6) (1990) 30.

[10] V. Kin, Topological Tolerancing of Worm-Gear Tooth Surfaces, American Gear Manufactures Association Conference, Virginia, 1993.
[11] V. Simon, J. Mech. Design 104 (1982) 731.
[12] W.L. Janninck, Gear Technology 5 (2) (1988) 31.